

## Internal magnetic field structure and parallel electric field profile evolution during the sawtooth cycle in MST

This article has been downloaded from IOPscience. Please scroll down to see the full text article.

2008 Plasma Phys. Control. Fusion 50 115013

(<http://iopscience.iop.org/0741-3335/50/11/115013>)

View [the table of contents for this issue](#), or go to the [journal homepage](#) for more

Download details:

IP Address: 128.104.166.214

The article was downloaded on 13/10/2010 at 22:35

Please note that [terms and conditions apply](#).

# Internal magnetic field structure and parallel electric field profile evolution during the sawtooth cycle in MST

B H Deng<sup>1</sup>, W X Ding<sup>1</sup>, D L Brower<sup>1</sup>, A F Almagri<sup>2</sup>, K J McCollam<sup>2</sup>,  
Y Ren<sup>2</sup>, S C Prager<sup>2</sup>, J S Sarff<sup>2</sup>, J Reusch<sup>2</sup> and J K Anderson<sup>2</sup>

<sup>1</sup> Department of Physics and Astronomy, University of California at Los Angeles, Los Angeles, CA 90095, USA

<sup>2</sup> Department of Physics, University of Wisconsin, Madison, WI 53706, USA

Received 13 August 2008, in final form 5 September 2008

Published 15 October 2008

Online at [stacks.iop.org/PPCF/50/115013](http://stacks.iop.org/PPCF/50/115013)

## Abstract

Temporal dynamics of the magnetic field, parallel current density, parallel electric field and safety factor profiles in the core of a high-temperature reversed-field pinch plasma are experimentally resolved. Measurements are realized using a high-speed polarimeter–interferometer diagnostic which is employed to simultaneously determine the electron density, toroidal current density and poloidal magnetic field profiles. Combined with external magnetic measurements, these data allow determination of the equilibrium profile dynamics during individual sawtooth magnetic relaxation events. At the sawtooth crash, the  $E_{\parallel}$  profile has a large positive peak on-axis, and a negative peak of slightly smaller value near the reversal surface demonstrating the need for a dynamo to sustain the plasma equilibrium.

(Some figures in this article are in colour only in the electronic version)

## 1. Introduction

The spatial structure of the current density and magnetic field is a major determinant of plasma behavior in many configurations of magnetically confined plasmas. The current density gradient provides a free energy source to drive fluctuations in the magnetic field, while magnetic field shear, represented by the safety factor ( $q$ ) profile, provides a stabilizing force against fluctuations. In the reversed-field pinch (RFP), fluctuations not only drive transport of particles and energy across the confining magnetic field but also regulate the current density distribution through the dynamo effect. It is well known that dynamo is required for sustaining steady-state RFP plasmas [1]. Dynamo effects are manifested by the imbalance between the parallel electric field profile ( $E_{\parallel} \equiv \mathbf{E} \cdot \mathbf{B}/B$ ) and that required to drive plasma current ( $\eta J_{\parallel}$ )

where  $J_{\parallel} \equiv \mathbf{J} \cdot \mathbf{B}/B$  and  $\eta$  is the plasma resistivity. Therefore, time resolved measurements of the  $E_{\parallel}$  profile can reveal important information on the dynamo and its temporal dynamics.  $E_{\parallel}$  profiles are dominantly inductive and can be obtained from Faraday's law if time resolved magnetic field profile information is available [2].

RFP discharges often exhibit cyclical magnetic reconnection events with periodicity of several milliseconds, also referred to as sawteeth. These are discrete dynamo events during which toroidal magnetic field is generated and rapid ( $\Delta t \sim 100\text{--}200 \mu\text{s}$ ) changes occur in the magnetic field and current density profiles. Previous measurements of the RFP internal magnetic field structure and current density distribution used ensembled data averaged over many sawtooth events where the density and magnetic field were measured independently for separate discharges [3, 4].

In this paper, we present measurements of the internal magnetic field structure and current density distribution during individual sawtooth events in the Madison Symmetric Torus (MST) RFP. Profiles of toroidal current density ( $J_{\text{tor}}$ ) and poloidal magnetic field ( $B_{\text{pol}}$ ) are measured by a far-infrared (FIR) laser polarimeter–interferometer system providing simultaneous density and magnetic field information with high time and phase resolution [5]. In addition, by using a simplified equilibrium analysis approach, information on the toroidal magnetic field ( $B_{\text{tor}}$ ) and safety factor profile ( $q = (r/R)(B_{\text{tor}}/B_{\text{pol}})$ ) evolution is obtained (where  $r$  corresponds to torus radial position in minor radius and  $R$  the major radius). From this information, the inductive  $E_{\parallel}$  profile during the sawtooth cycle can also be resolved. As an independent measure of accuracy, the inferred value of the toroidal field at the magnetic axis agrees well with its value measured by a motional Stark effect (MSE) diagnostic [6].

We find that the safety factor profile exhibits a sawtooth-like modulation where the value on axis increases by  $\sim 20\%$  at each crash.  $J_{\parallel}(0)$  collapses at the crash, recovering slowly during the linear-ramp phase. The current density profile shape is observed to be essentially invariant when raising the plasma current from 180 to 580 kA. However, current channel narrowing is observed when the RFP plasma becomes more deeply reversed. Excellent temporal resolution of the magnetic field profile measurements makes it possible to calculate the inductive electric field profiles over a sawtooth cycle. It is found that between sawtooth crashes,  $E_{\parallel}$  is small and its profile is peaked off-axis while the plasma current density profile peaks on-axis. At a sawtooth crash, when the current profile is flattened,  $E_{\parallel}$  profiles are characterized with a large positive central peak and a large negative peak near the reversal radius. When averaged over the sawtooth cycle, the  $E_{\parallel}$  profile is centrally peaked, with the maximum value determined by the externally applied loop voltage, consistent with the intuitive expectation based on steady-state current sustainment [1]. An imbalance between measured parallel electric field profile and product of plasma parallel current and resistivity over the sawtooth cycle indicates the need for dynamo in order to satisfy Ohm's law.

This paper is organized as follows: in section 2, the equilibrium analysis method employed is described; in section 3, magnetic and current density profile dynamics along with scaling are presented; in section 4, the parallel electric field profile temporal evolution during a sawtooth cycle is shown; and section 5 contains a discussion and a summary of experimental results.

## 2. Equilibrium model and measurement approach

RFP plasmas tend to relax toward a force free configuration, where plasma current is parallel to magnetic field, i.e.  $J_{\text{pol}} = \lambda B_{\text{pol}}/(\mu_0 a)$ ,  $J_{\text{tor}} = \lambda B_{\text{tor}}/(\mu_0 a)$  and  $\lambda \equiv \mu_0 a J_{\parallel}/B$  is constant (where  $a$  is plasma minor radius). This tendency, together with Ampere's law, couples the poloidal and toroidal magnetic field profiles making it possible to derive  $B_{\text{tor}}$  ( $J_{\text{pol}}$ ) profiles from  $B_{\text{pol}}$  ( $J_{\text{tor}}$ ) profiles.

It was shown previously that poloidal magnetic field (and  $J_{\text{tor}}$ ) profiles can be measured with high-time resolution using the multi-chord FIR laser polarimeter–interferometer diagnostic in MST [3–5, 7]. In order to also obtain  $B_{\text{tor}}$  profiles using this information, two practical situations need to be considered. First, a current component perpendicular to the magnetic field is required to balance plasma pressure. Second, the perfect conductor boundary condition requires the current to vanish there. The latter forces  $\lambda$  to have a spatially varying profile, for example,  $\lambda(r) = \lambda_0(1 - (r/a)^\alpha)$ . This  $\lambda$ -profile is used in the so-called alpha model to calculate the equilibrium magnetic profiles using only  $I_p$ ,  $B_{\text{tor}}(a)$  and  $\overline{B}_{\text{tor}}$  from external magnetic measurements and assuming a parabolic pressure profile [8].

Herein, we use a different method to determine the equilibrium profiles. From Ampere’s law,  $\nabla \times \vec{B} = \mu_0 \vec{J}$ , and the definition  $\lambda \equiv \mu_0 a J_{\parallel} / B$ , in a cylindrical co-ordinate system it can be shown that

$$\frac{dB_{\text{tor}}}{dr} = -\frac{\lambda}{a} \frac{B_{\text{tor}}^2 + B_{\text{pol}}^2}{B_{\text{pol}}} + B_{\text{tor}} \left( \frac{1}{r} + \frac{1}{B_{\text{pol}}} \frac{dB_{\text{pol}}}{dr} \right). \quad (1)$$

By using the measured  $B_{\text{pol}}$  profile, this differential equation can be solved numerically to obtain the  $B_{\text{tor}}$  profile. The two free parameters in the  $\lambda$ -profile ( $\lambda_0$  and  $\alpha$ ) are determined iteratively in the solving process by adding two additional constraints,  $B_{\text{tor}}(a)$  and average value of  $B_{\text{tor}}$  ( $\overline{B}_{\text{tor}}$ ), measured by external magnetic coils.

In obtaining the poloidal magnetic field (and  $J_{\text{tor}}$ ) profiles from measurements of Faraday rotation and density, toroidal effects are included by using the shifted circular flux surface approximation [3–5]. Once equation (1) is solved for profiles of  $\lambda(r)$  and  $B_{\text{tor}}$ , one can readily obtain the spatial distribution of  $J_{\parallel}$  and safety factor,  $q$ . This two-step approach, referred to herein as FIRfit, uses internal constraints imposed by the interferometer–polarimeter measurements along with the external magnetic measurements of  $I_p$ ,  $B_{\text{tor}}(a)$  and  $\overline{B}_{\text{tor}}$ . Interferometer–polarimeter system time response of  $\sim 4 \mu\text{s}$  provides excellent temporal resolution allowing the fast time evolution of the  $B_{\text{pol}}$ ,  $B_{\text{tor}}$ ,  $q$  and  $J_{\parallel}$  profiles to be determined. Previous measurements of the toroidal current and poloidal magnetic field in MST [3, 4] were obtained by operating the diagnostic as an interferometer or polarimeter separately and then combining the datasets by ensemble averaging over many sawtooth events. For results presented herein, the system was upgraded so that simultaneous interferometry and polarimetry measurements [5] were possible, thereby allowing us to investigate individual sawtooth events for a given discharge.

Full modeling of the MST internal magnetic field structure is achieved using the equilibrium reconstruction code MSTfit [9] which provides a toroidal equilibrium solution best fitting all of the magnetic (external and internal) and pressure data available. However, high-time resolution pressure measurements are not available during individual sawtooth cycles for a given discharge. Compared with MSTfit, FIRfit does not depend on plasma pressure measurements thereby improving the time resolution. Instead, FIRfit uses the simplified two-parameter model,  $\lambda = \lambda_0(1 - (r/a)^\alpha)$ , to describe the RFP plasma equilibrium. Neither MSTfit or FIRfit uses helicity conservation as a constraint on the equilibrium reconstruction. However, evaluation of the helicity shows that it is conserved during the sawtooth cycle [9]. By directly comparing profiles obtained using the two approaches (section 3), we will establish that the treatment provided in FIRfit is suitable for the application presented.

All measurements reported herein are made on the MST RFP device [10] which has a major radius  $R_0 = 1.5 \text{ m}$  and minor radius  $a = 0.51 \text{ m}$ . For the standard sawtoothed plasmas investigated, plasma current ( $I_p$ ) ranges from 180 to 580 kA, and line-averaged density is typically  $\sim 10^{19} \text{ m}^{-3}$ . All data presented are obtained during the current flat-top periods of the standard plasma discharges. Specific examples of the interferometry and polarimetry

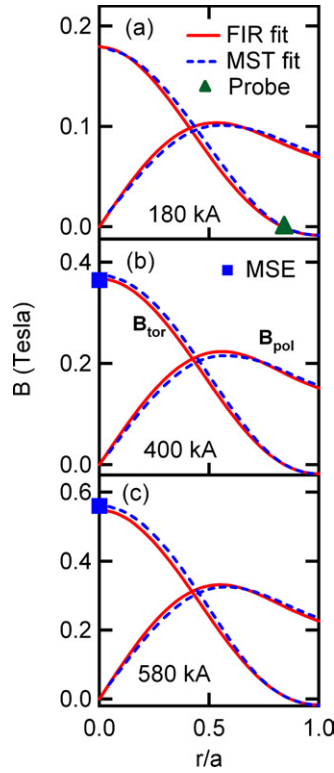


**Figure 1.** Comparison of magnetic field profiles from FIRfit (solid curves) with MSTfit (dashed curves), MSE data (squares), and probe data (triangles) for (a) 180 kA, (b) 400 kA and (c) 580 kA standard discharges.

time series data and profiles as well as description of the measurement technique have been previously published and will not be shown here [3–5, 7].

### 3. Magnetic and current density profile scaling and temporal dynamics

The suitability of the FIRfit approach for standard MST plasmas is established by comparison of the magnetic field profiles thus obtained with those from the MSTfit analysis as shown in figures 1(a)–(c), for discharges with  $I_p = 180$  kA, 400 kA and 580 kA, respectively. Profiles are evaluated at the midway point of the sawtooth cycle and the reversal parameter  $F = B_{\text{tor}}(a)/\bar{B}_{\text{tor}} \approx -0.15$  for these discharges. In these figures, the solid curves are obtained using FIRfit and the dashed curves are obtained from MSTfit. For each case, the difference between the reconstructed profiles is within experimental errors, which typically range from 10–20% for 180 kA discharges to 5–10% for 580 kA discharges. The relative error is larger at smaller plasma current due to smaller Faraday rotation angles.

In figures 1(b) and (c), a  $B_{\text{tor}}$  data point (solid square) near the magnetic axis ( $B_0$ ) measured by a MSE diagnostic is also shown. MSE measurements are only made at the magnetic axis. Here we see the directly measured value for  $B_0$  agrees very well with the result of FIRfit. For low current discharges (figure 1(a)), MSE measurements are not available due to small signal to noise ratio. However, at low current the FIRfit reversal radius position (i.e. point in space where  $B_{\text{tor}}$  goes to zero),  $r/a \sim 0.85$ , matches that measured by magnetic probes as shown

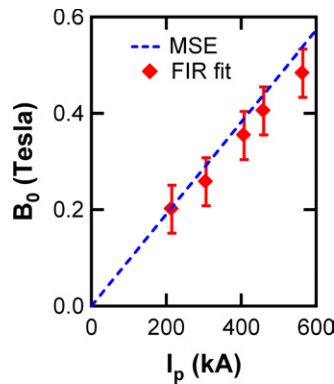


**Figure 2.**  $B_0$  increases with plasma current. Solid diamonds (red) are from FIRfit and the dashed line (blue) represents a fit to MSE measurements of  $B_0$ .

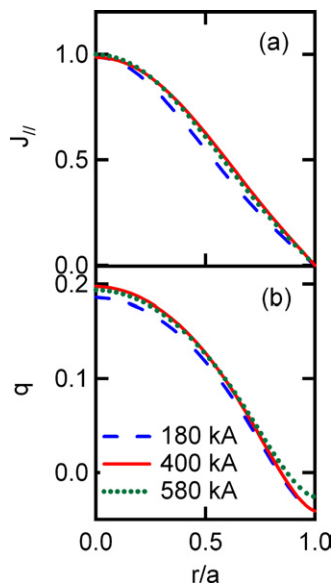


**Figure 3.** (a) Normalized parallel current and (b)  $q$  profiles for  $I_p = 180$  (long dash—blue), 400 (solid—red), and 580 kA (short dash—green). The values of  $J_{||}(0)$  are 1, 2 and 3  $\text{MA m}^{-2}$  for  $I_p = 180$  kA, 400 kA and 580 kA, respectively.

in figure 1(a). Under various plasma conditions,  $B_0$  obtained from FIRfit agrees with MSE measurements of  $B_0$  to within 5% and with dependence on  $I_p$  to within  $\sim 10\%$ , as shown in figures 1 and 2, respectively. The variation of  $B_0$  with plasma current reflects the fact that in RFP plasmas, the source of toroidal flux is the externally applied poloidal flux. Agreement between the two reconstruction approaches and MSE measurements establishes that the FIRfit model is suitable for determining the MST equilibrium profiles for standard plasmas.

For the same conditions shown in figure 1, the corresponding parallel current density and  $q$  profiles are shown in figure 3. While the current density on axis increases with plasma current from 1 to 3  $\text{MA m}^{-2}$ , as expected, the profile shape is essentially constant within experimental error ( $< 10\%$ ). In addition, since  $B_0$  also increases with current, as previously mentioned, the  $q$  profile is observed to remain unchanged with variation in plasma current. However,

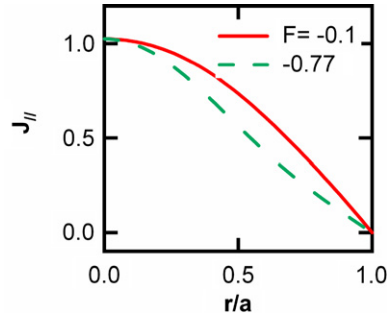


**Figure 4.** Parallel current density profile changes with reversal parameter  $F$ . Values on axis have been normalized to 1.

the current profile shape can be modified by changing the reversal parameter  $F$  as shown in figure 4. Here we see that as  $F$  becomes more negative (and the  $B_{\text{tor}}$  reversal radius moves inward), the current profile narrows.

Excellent time resolution provided by the FIR polarimeter–interferometer diagnostic makes it possible to follow the temporal evolution of magnetic field profiles over a sawtooth cycle for individual events. Time traces of the on-axis magnetic field ( $B_0$ ), current density ( $J_0$ ) and safety factor ( $q_0$ ) over consecutive sawtooth cycles of a 400 kA standard discharge are shown in figure 5. The time resolution used in the FIRfit is 0.1 ms. The slow increase of  $J_0$  indicates current profile peaking on axis during the linear-ramp phase, and the sudden decrease of  $J_0$  (although total current  $I_p$  increases) signifies the current profile flattening at a sawtooth crash, consistent with previous measurements [3, 4]. At each crash,  $q_0$  jumps to above 0.2, so that the  $m = 1, n = 5$  mode becomes resonant at the core. However, the mode quickly becomes non-resonant when  $q_0$  decreases to below 0.2 as the current profile begins to peak. During the entire sawtooth cycle, the  $m = 1, n = 6$  mode is resonant in the plasma core. This is consistent with observations that the (1, 6) mode is the dominant mode in MST as determined from magnetic fluctuation measurements [10]. As  $q_0$  decreases, approaching  $\sim 1/6$ , a sawtooth crash occurs. The increase in  $q(0)$  at the sawtooth crash is consistent with the decrease in  $J(0)$  and flattening of the current profile.

As shown in figure 5, the on-axis ( $B_0$ ) magnetic field is also sawtoothing. This is consistent with direct measurements by MSE in the plasma core [6], and expectations from 3D MHD simulation [11]. Both the core and edge values of  $B_{\text{tor}}$  decrease at the sawtooth crash, however, the average toroidal magnetic field ( $\bar{B}_{\text{tor}}$ ) increases, as shown in figure 3(e), due to the plasma dynamo effect. Therefore,  $B_{\text{tor}}$  values at mid-radius must increase as predicted by 3D MHD simulations [13] and confirmed by the surface plot of  $B_{\text{tor}}$  profile evolution over a single sawtooth cycle, as shown in figure 6.

For the discharges shown in figure 5, the FIRfit quantities ( $B_0, J_0, q_0$ ) evidence a minor crash at  $\sim 24$  ms, which is correlated with the (1, 6) mode amplitude ( $|\tilde{B}_p|$ ) change (see figure 5(f)). This is a core localized event, which is detected by the central FIR channels, as shown in the time trace (figure 5(d)) of the Faraday rotation angle ( $\psi_F$ ) measured by a FIR polarimetry channel with the laser beam passing near the resonant radius of the (1, 6) mode. Edge measurements of  $B_t(a)$  and  $\bar{B}_{\text{tor}}$  do not record this core event, illustrating the sensitivity of the FIR diagnostic and the advantage of having core measurements of the internal field structure.

Further illustrating the change in profiles at a reconnection event,  $B_{\text{tor}}, B_{\text{pol}}, J_{\parallel}$  and  $q$  profiles measured before (27.7 ms) and after (28 ms) a sawtooth crash are shown in figure 7. Before a sawtooth crash, the  $J_{\parallel}$  profile is very peaked, and then flattens significantly after the

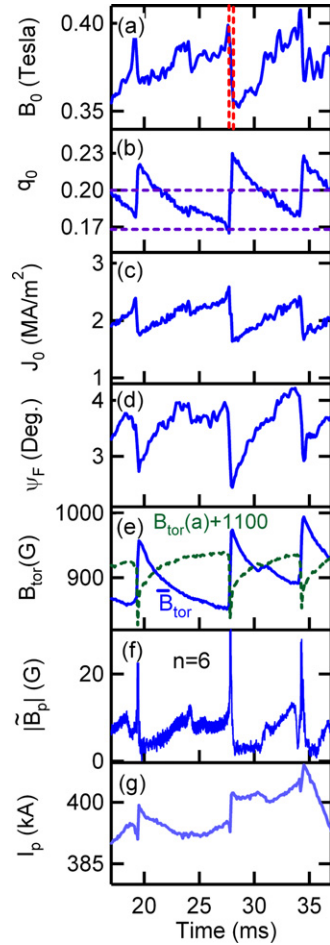


**Figure 5.** Time traces from a single 400 kA standard discharge where (a)  $B_0$  (vertical dashed lines correspond to time selected for profiles in figure 7), (b)  $J_0$  and (c)  $q_0$  are the on axis equilibrium magnetic field, current density, and safety factor, respectively, (d)  $\psi_F$  is the Faraday rotation angle measured by a FIR polarimetry chord passing near the resonant radius of the (1, -6) mode, (e)  $B_{\text{tor}}$  (a) and  $\bar{B}_{\text{tor}}$  are the edge and average toroidal magnetic field, respectively, (f)  $|\tilde{B}_p|$  is the (1, 6) mode amplitude and (g)  $I_p$  is the total plasma discharge current.

crash. The more peaked current profile before the crash, with correspondingly lesser magnetic shear, tends to be linearly destabilizing, although nonlinear physics is known to be important throughout the relaxation process. With the high-time resolution of FIRfit, it is now feasible to test the dynamic changes of plasma stability under various plasma discharge conditions.

#### 4. Electric field profile dynamics

RFP plasmas are partly self-sustained by the dynamo effect, which is a fluctuation-driven electromotive force that can modify the electric field profile. Temporally resolved measurements of electric field profiles can reveal information on the dynamo field spatial distribution and evolution by looking at the imbalance between  $E_{\parallel}$  and  $\eta J_{\parallel}$  in Ohm's law. Generally, when time resolved magnetic field profiles are known, the inductive electric field

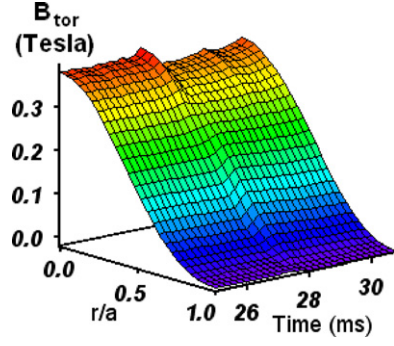


**Figure 6.** Evolution of  $B_{\text{tor}}$  profiles over a single sawtooth event in a 400 kA standard discharge. The time traces of the on-axis value ( $B_0$ ), edge value ( $B_{\text{tor}}(a)$ ) and space average value ( $\bar{B}_{\text{tor}}$ ) are shown in figure 5.

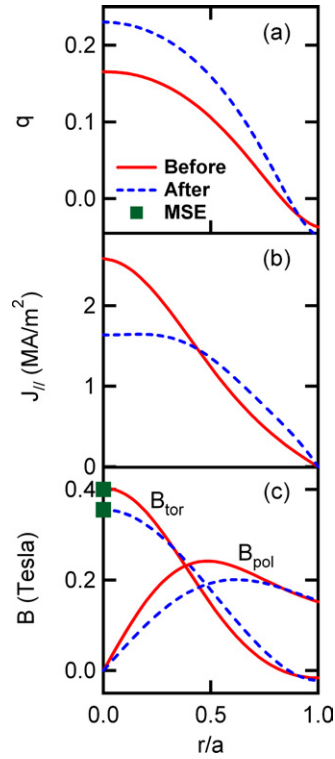


**Figure 7.** Equilibrium profiles before (27.7 ms, solid curves) and after (28 ms, dashed curves) a sawtooth crash in a 400 kA discharge. Time slices selected correspond to vertical dashed lines in figure 5(a). MSE measurements of  $B_0$  taken from [11] are denoted by solid squares.

profiles can be determined from Faraday's law according to [2]

$$E_{\text{tor}}(r) = E_{\text{tor}}(a) - \int_r^a \frac{\partial}{\partial t} B_{\text{pol}} dr', \quad (2)$$

$$r E_{\text{pol}}(r) = a E_{\text{pol}}(a) + \int_r^a \frac{\partial}{\partial t} B_{\text{tor}} r' dr' = - \int_0^r \frac{\partial}{\partial t} B_{\text{tor}} r' dr'. \quad (3)$$

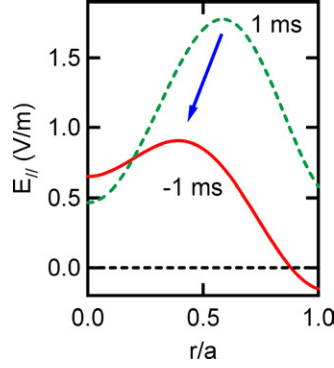


**Figure 8.** Parallel electric field profiles at 1 ms before (solid curve) and 1 ms after (dashed curve) the sawtooth crash for 400 kA standard discharges. Each profile is smoothed over 0.3 ms time window.

Here,  $E_{\text{tor}}(a)$  and  $E_{\text{pol}}(a)$  are the toroidal and poloidal electric fields at the plasma surface, determined from the toroidal and poloidal loop voltages, respectively.

For standard RFP plasma discharges in MST with  $I_p = 400$  kA, the sawtooth period typically varies from 4 to 8 ms. To reduce random errors, ensemble averaging is performed to obtain the time evolution of magnetic field profiles from  $-2.5$  ms (before) to  $+2.5$  ms (after) a sawtooth crash. The ensemble consists of 80 sawtooth events, each selected during the current flat-top period of discharges displaying sawtooth period of  $5 \pm 1$  ms. Time resolved electric field profiles are subsequently calculated (every 0.1 ms) using equations (2) and (3). Shown in figure 8 are the parallel electric field profiles at times 1 ms before (solid curve, labeled ‘ $-1$  ms’) and 1 ms after (dashed curve, labeled ‘ $1$  ms’) sawtooth crash. The profile change from  $+1$  to  $-1$  ms characterizes the general trend of  $E_{\parallel}$  evolution during the sawtooth linear-ramp phase. After a sawtooth crash ( $+1$  ms),  $E_{\parallel}$  peaks at  $r/a \sim 0.6$  and is hollow. This hollow profile shape is consistent with peaking of current density profile on axis. From Faraday’s law,  $\nabla \times \mathbf{E} = -\partial \mathbf{B} / \partial t$ , we have  $\partial E_z / \partial r = \partial B_{\text{pol}} / \partial t$ . In the plasma core ( $r \ll a$ ),  $B_{\text{pol}} (\sim r J_0)$  increases with time when current density is peaking on axis. Therefore,  $\partial E_z / \partial r > 0$ , leading to the hollow  $E_{\parallel}$  profile seen in figure 8. In the plasma core, the  $E_{\parallel}$  value is close, within error, to that required to match the resistive electric field ( $\eta J_{\parallel}$ ) of  $\sim 0.5$ – $1$  V m $^{-1}$  (see figure 1 in [12]). This implies that during the sawtooth ramp phase, little or no dynamo is required in the plasma core, consistent with previous dynamo measurements [13]. A sawtooth crash is a discrete dynamo event during which the current profile is flattened, i.e.  $J_0$  decreases by  $\sim 20$ – $30\%$  in  $\sim 100$ – $200$   $\mu$ s, while the edge current density increases. From Lenz’s law, the inductive electric field will react to oppose the current profile change caused by dynamo electromotive force. Therefore, the electric field profile develops a large positive peak in the core and a large negative peak near the reversal radius, as shown in figure 9. The core plasma inductive electric field ( $\sim 40$  V m $^{-1}$ ) must be balanced by the dynamo electromotive force since the resistive electric field is small ( $< 1$  V m $^{-1}$ ). This is true in the plasma core since the on-axis value of  $E_{\parallel}$ , shown in figure 9, is comparable to the dynamo electromotive force obtained from Hall dynamo ( $\tilde{\mathbf{j}} \times \tilde{\mathbf{b}}$ ) measurement [14, 16]. At the plasma edge, previous spectroscopic measurements have shown that the electric field is balanced by the MHD dynamo ( $\tilde{\mathbf{v}} \times \tilde{\mathbf{b}}$ ) electromotive force [13, 16].

By taking the average of all the profiles generated during the sawtooth cycle (i.e. one profile every 0.1 ms), the mean toroidal (long dashed curve), poloidal (dotted curve), and parallel (solid curve) electric field profiles are obtained and shown in figure 10. These profiles

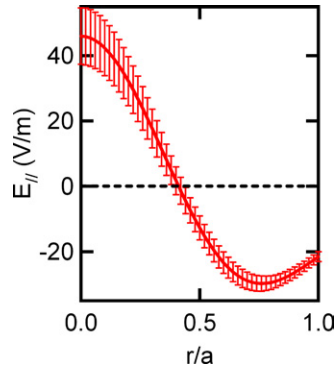


**Figure 9.** Parallel electric field profile at the sawtooth crash of 400 kA discharges, averaged from  $-0.05$  to  $0.05$  ms. Profile is averaged over  $0.1$  ms time window.

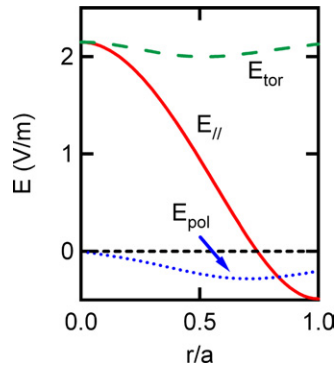


**Figure 10.** Toroidal (long dashed curve), poloidal (dotted curve) and parallel (solid curve) electric field profile for 400 kA standard discharges.

reflect the quasi-stationary conditions ( $15 < t < 35$  ms) where  $I_p$  varies by less 5% (see figure 5(g)). From equation (2), it is expected that  $E_{\text{tor}}(r) = E_{\text{tor}}(a)$  is a constant across the plasma column for this quasi-steady period, with  $E_{\text{tor}}(a) = V_{\text{tor}}/2\pi R_0$ , where  $V_{\text{tor}}$  is the toroidal loop voltage applied at the plasma surface (by the Ohmic transformer). This is confirmed by the long dash curve in figure 10, where  $E_{\text{tor}} \sim 2 \text{ V m}^{-1}$  and constant within error bars. Similarly, from equation (3),  $E_{\text{pol}}$  should be near zero for this quasi-steady period, consistent with the very small sawtooth-averaged  $E_{\text{pol}}$  shown in figure 10 (dotted curve). The parallel electric field (solid curve) is predominantly the projection of the constant toroidal electric field in the magnetic field direction, and therefore, it is similar in shape to the toroidal magnetic field profile. This centrally peaked  $E_{\parallel}$  profile is quite different from the resistive electric field ( $\eta J_{\parallel}$ ) profile (see figure 1 of [12]), which is flat and  $\sim 0.5 \text{ V m}^{-1}$  for  $r/a < 0.9$ , supporting the claim that dynamo is required to sustain RFP plasmas [1].

## 5. Discussion and summary

Simultaneous, high-speed, polarimetry–interferometry measurements in combination with the FIRfit equilibrium analysis have been used to determine the internal magnetic field structure and its temporal evolution during the sawtooth cycle in MST. Comparisons show  $B_0$  obtained

using FIRfit is in excellent agreement with direct MSE measurements at the magnetic axis. Results from FIRfit also match well with those from the full equilibrium analysis MSTfit. This is not surprising because the two parameter model  $\lambda = \lambda_0(1 - (r/a)^\alpha)$ , first used in the alpha model, is generally believed to be well suited for describing the RFP equilibrium, and confirmed from probe measurements in low current smaller RFP device [8].

With the high temporal and phase resolution data provided by the FIR interferometer-polarimeter measurements, the magnetic profile dynamics for sawtooth high-temperature MST RFP plasmas are examined for discrete reconnection events. A sawtooth response is observed in the profiles of  $B_{\text{pol}}$ ,  $B_{\text{tor}}$ ,  $J_{\parallel}$  and  $q$ . Crashes tend to occur when  $q(0)$  approaches  $1/6$ , corresponding to the disappearance of resonant surface for the dominant core resonant mode, as predicted by MHD simulations [12]. The parallel current profile shape is observed to be relatively invariant as the plasma current is scanned from 180 to 580 kA for fixed reversal parameter. In addition, self-generation of toroidal field via the dynamo mechanism must rise with plasma current in order to maintain a constant  $q$  profile as is measured. Marginal stability of MHD modes (which provide the dynamo driving mechanism) may act as a clamping mechanism leading to stiffness of the current and  $q$  profiles. However,  $J_{\parallel}$  profile does narrow when the reversal parameter becomes more negative. During the slow linear sawtooth ramp phase, the parallel electric field profile is hollow at the plasma core, peaking near half radius, with little or no dynamo required to match the resistive electric field. At the sawtooth crash, for a period of  $<0.2$  ms, the  $E_{\parallel}$  profile has a large positive peak on axis, and a negative peak of slightly smaller value near the reversal surface denoting the need for a dynamo emf.

### Acknowledgment

This work is supported by the US Department of Energy under Grant No DE-FG02-01ER54615.

### References

- [1] Ho Y L, Prager S C and Schanack D D 1989 *Phys. Rev. Lett.* **62** 1504
- [2] Hutchinson I H 1987 *Principles of Plasma Diagnostics* (Cambridge: Cambridge University Press)
- [3] Brower D L, Ding W X, Terry S D, Anderson J K, Biewer T M, Chapman B E, Craig D, Forest C B, Prager S C and Sarff J S 2002 *Phys. Rev. Lett.* **88** 185005
- [4] Terry S D *et al* 2004 *Phys. Plasmas* **11** 1079–86
- [5] Deng B H, Brower D L, Ding W X, Wyman M D, Chapman B E and Sarff J S 2006 *Rev. Sci. Instrum.* **77** 10F108
- [6] Den Hartog D J *et al* 2006 *Rev. Sci. Instrum.* **77** 10F122
- [7] Brower D L, Ding W X, Terry S D, Anderson J K, Biewer T M, Chapman B E, Craig D, Forest C B, Prager S C and Sarff J S 2003 *Rev. Sci. Instrum.* **74** 1534
- [8] Ortolani S and Schnack D D 1993 *Magnetohydrodynamics of Plasma Relaxation* (Singapore: World Scientific)
- [9] Anderson J K, Forest C B, Biewer T M, Sarff J S and Wright J C 2004 *Nucl. Fusion* **44** 162
- [10] Prager S C *et al* 1990 *Phys. Fluids* **B 2** 1367–71
- [11] Kusano K and Sato T 1990 *Nucl. Fusion* **30** 2075
- [12] Anderson J K *et al* 2005 *Phys. Plasmas* **12** 056118
- [13] Den Hartog D J, Chapman J T, Craig D, Fiksel G, Fontana P W, Prager S C and Sarff J S 1999 *Phys. Plasmas* **6** 813
- [14] Ding W X, Brower D L, Terry S D, Craig D, Prager S C, Sarff J S and Wright J C 2003 *Phys. Rev. Lett.* **90** 035002
- [15] Ding W X, Brower D L, Craig D, Deng B H, Fiksel G, Mirnov V, Prager S C, Sarff J S and Svidzinski V 2004 *Rev. Lett.* **93** 045002
- [16] Fontana P W, Den Hartog D J, Fiksel G and Prager S C 2000 *Phys. Rev. Lett.* **85** 566